Size effect of concrete and sandstone

Marcel R.A. van Vliet
TNO Building and Construction Research, Lange Kleiweg 5, P.O. Box 49,
2600 AA Delft, the Netherlands

Jan G.M. van Mier
Delft University of Technology, Faculty of Civil Engineering and Geosciences,
P.O. Box 5048, 2600 GA Delft, the Netherlands

A series of uniaxial tension experiments has been conducted to investigate the size effect on strength and fracture energy of concrete and sandstone. The experiments were carried on specimens of six different sizes in a scale range of 1:32. Depending on the material and the curing conditions a stronger or weaker size effect on the nominal strength occurred in the tests. The observed size effect was attributed to a combination of statistical size effect and strain gradients in the cross section of the specimens, which were caused by the specimen shape, load eccentricity and material inhomogeneity. The fracture energy was, irrespective of the type of material, found to increase with size going towards a horizontal asymptote for large sizes.

Key words: **size effect, concrete, sandstone, Weibull theory, stress/strain gradients**

1 Introduction

In the field of civil engineering, laboratory experiments are a frequently used tool to get insight in the behaviour of structural details or the materials they are composed from. If the material under investigation is concrete or rock, the structural sizes that have to be dealt with easily exceed the maximum size that can still be tested in a laboratory. For this reason such experiments are often scaled versions of reality. It is known that this scaling can induce a size dependence of the experimental result, i.e. the result depends on the size of the specimen that was tested. A thorough knowledge of this size effect is therefore needed to be able to translate the experimental numbers to values that can be applied in engineering practice.
As a contribution to current and previous research dealing with size effect, a combined experimental and numerical investigation was started to study size effect in concrete and sandstone under uniaxial tension. These uniaxial tensile loading conditions were chosen because they constitute the most basic failure mechanism of quasi brittle materials, thereby offering the best possibility to study a size effect of the material itself. Structural effects, which in addition to material effects will always be present in the experimental result, are minimised while applying rotating boundary conditions. The experiments were carried out under deformation control, so that a size effect on the nominal strength as well as the fracture energy could be studied.

In this paper the size effect on the nominal strength and fracture energy is discussed. Observations from laboratory experiments are presented, with as main goal getting insight in the physical mechanisms underlying the observed size effect. First an outline is given of the experimental set-up. Thereafter, the results of uniaxial tension tests on concrete specimens are given, which comprised a series of specimens cured in the laboratory ("DRY" series) as well as a series of specimens cured in the climate room ("WET" series), followed by the results of the sandstone tests. At the end of the paper it will be shown that the strength of part of the concrete tests followed classical Weibull theory, whereas the presence of stress and/or strain gradients caused the remaining size effect on strength.

2 Outline of experiments

2.1 *Specimens and material properties*

When studying material size effect it would be most natural to use specimens scaled in three dimensions, or at least scaled in two dimensions but with a prismatic cross section. Besides theoretical demands however, practical needs have to be considered as well, which resulted in the choice for dog-bone shaped specimens as shown in Fig. 1 (Van Vliet, 2000). From the dog-bone shape a non-uniform stress state develops within the specimens, similar to specimens in which notches are applied. The tests are still referred to as uniaxial tension tests however, since failure of the specimens takes place under mode I loading conditions. The effects of the non-uniform stress-state are incorporated in the analysis of the experimental results.

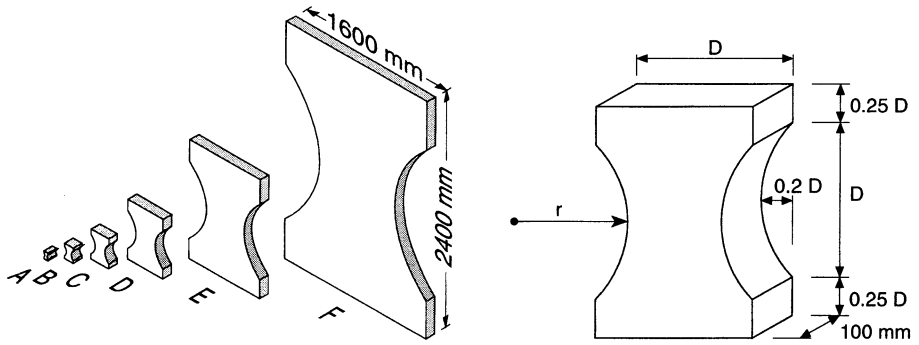

Fig. 1. Specimens with sizes in a scale range of 1:32 and specimen proportions.

type	A	B	C	D	E	F
D [mm]	50	100	200	400	800	1600
r [mm]	36.25	72.5	145	290	580	1160

Circular bays reduce the cross section in the middle of the specimen with 40% compared to the specimen ends so that glue problems can be avoided. The use of circular bays instead of notches is thereby preferred for several reasons. These are smaller stress concentrations, a more straightforward way of scaling and easier reproducibility without introducing damage during manufacturing. An even more important advantage of dog-bone shaped specimens is the fact that the area where failure can occur is larger compared to notched specimens. Failure is therefore more likely to occur at the weakest spot in the material, rather than being induced in a narrow zone with large stress concentrations whose influence on the ultimate load can only be guessed. As for the global dimensions of the specimens, the height to width ratio was fixed at 1.5 to ensure that in the middle of the specimen boundary influences have averaged out.

Table 1. Concrete mix properties.

Unit content kg/m^3							
8–4*	4–2*	2–1*	1–0.5*	0.5-0.25*	0.25-0.125*	PCB	w/c
540	363	272	272	234	127	375	0.5

*aggregate size in mm, PCB: Portland Cement type B, w/c: water cement ratio

A concrete mixture was applied with an average cube compressive strength of 50 MPa and $d_{max} = 8$ mm. The composition is shown in Table 1. Based on the maximum grain diameter of 8 mm the outer dimensions of the smallest specimen were taken 50 × 75 mm. Although the resulting minimal width of 30 mm is rather close to the common rule that the smallest structural dimension should be taken 3 to 5 times larger than the maximum aggregate size, it was decided that the results had to show whether 30 mm is too small. The thickness of the specimens was set at a constant value of 100 mm. Fig. 1 illustrates the test range of 1:32 that resulted from scaling the smallest specimen in two directions, as well as the final specimen dimensions. Note that by keeping a constant thickness the state of stress in the type **A** specimen tends to a plane-strain situation. In different words, a shape effect is introduced, but it should be realised that this is the case in almost every experimental study on size effects reported in literature. This effect remains, however, generally "un-detected".

In addition to the concrete experiments a series of uniaxial tension tests was carried out on specimens consisting of a completely different material. Based on good experiences in the past, red Felser sandstone was chosen which was retrieved from a quarry in Germany, north of Kaiserslautern. The sandstone is very homogeneous, although the mechanical behaviour is transversely isotropic due to the clear presence of bedding layers in the material (Van Vliet, 1997). For this reason all specimens were manufactured and loaded in the same direction, namely parallel to the bedding layers. As for the composition, the sandstone consists of quartz grains with diameters between 0.2 and 0.6 mm that are embedded in a clay matrix. The unconfined compressive strength of the airdried sandstone is 41 MPa in average, when applying the load parallel to the bedding layers.

2.2 *Experimental set-ups and control system*

Numerous studies previously carried out (see e.g. Van Mier et al., 1995) showed that the outcome of a uniaxial tension test will be strongly affected by boundary influences when keeping the specimen ends parallel to each other during the test. When the specimen ends can rotate freely on the other hand, these boundary influences are minimised yielding among others a lower bound for the fracture energy.

Performing uniaxial tension tests with these so called rotating boundary conditions, was one of the starting points of the experiments. In order to create rotating boundary conditions a special hinge construction was developed to ensure free rotations of the specimen ends in two orthogonal directions. Moreover, the point of rotation is situated exactly in the glue layer between specimen and loading platen (Van Vliet, 2000).

Conducting all tests in one single test set-up was not practically feasible. It was therefore decided to carry out the tests in three different test frames, each with its own hinge construction (Van Vliet, 2000). When using different frames however, the risk was present for stiffness differences among the frames influencing the experimental result. To take this into account, specimen type **C** was tested in both the smallest and the middle-sized frame. By testing specimen type **D** in both the middle-sized frame and the large frame, differences between these two frames could be eliminated as well. Generally, these stiffness influences originating from testing specimens in two different loading frames are neglected. The results of the verification tests revealed that test stability decreases, and that structural effects affect the experimental result when the size of the specimens becomes too small with respect to the size of the set-up. Yet, correction of the results of the main test series based on these findings was not only found to be difficult, it would probably also lead too far (Van Vliet, 2000).

Inherent to the specimen shape is the fact that the area where crack initiation can occur, scales with the size of the specimen. In order to control the tests on the largest specimens as well, special care has to be taken. A possibility would be to scale the measuring length of the control LVDT with the specimen size. Hordijk (1991) however, clearly showed the increasing risk of snap-back behaviour at peak load with an increase in the measuring length. Also from the tension tests carried out by Ferro (1994) it can be concluded that the measuring length cannot be increased in an unlimited way. To eliminate the risk of running into snap-back problems caused by a too large measuring length, a small and constant measuring length was adopted in combination with a type of test control similar to that proposed by Li et al. (1993). On both the front and the back side of the specimen linear variable displacement transducers (LVDTs) with a measuring length of 75 mm were placed in line above each other. A specially developed control device checked, continuously, up to sixteen LVDTs to find the LVDT measuring the largest deformation. This LVDT was used to control the test. If at some later instant another LVDT measured a larger deformation, test-control was switched automatically to that LVDT. In preliminary tests preceding the final test series also other types of test-control were studied, like taking the average signal of two or four LVDTs as control signal. It was found, however, that controlling the test by means of the maximum deformation measured at a certain time and location, was the best guarantee for stable post-peak specimen behaviour (Van Vliet,

2000). For the largest specimen the total number of sixteen LVDTs was divided in two groups of eight, placed on the left front and the left rear side of the specimen. Therefore, it had to be ensured that the crack actually initiated at the left side of the specimen. This was achieved by applying a small load-eccentricity. The eccentricity, which was obtained by glueing the specimen eccentrically to the loading platens, was scaled according to the specimen size. In this way the (theoretical) linear elastic stress distribution in the middle of the specimen remains the same regardless of the size of the specimen. This is also reflected by the expression for the maximum stress σ_{max} in the specimen middle

$$\sigma_{max} = F/A[1 + 6e/(0.6D)],\ e = D/50\ \text{[mm]}$$

where A is the cross-sectional area, $0.6D$ the width of the smallest cross section and e the eccentricity of the external force F.

2.3 *Specimen preparation*

2.3.1 Concrete

All specimens were cast horizontally in three layers. After casting, each layer was compacted with a vibration needle. Since only five specimens of different size could be cast at a time, several weeks were needed for casting all specimens. Two days after casting the specimens were demoulded and stored under laboratory conditions (20°C, 50% R.H.) until the time of testing. All specimens have been tested at an age between 56 and 61 days, to ensure that the strength increase due to ongoing hydration was negligible. Three to seven days before testing the loading platens were glued to the specimen ends using a two-component epoxy resin. Finally, the measuring points were glued on the specimen surface, which concluded the test preparations. During a test the load was transferred to the specimen by bolts connecting the loading platens with the hinge construction.

The manufacturing procedure as described above applies to the concrete specimens of the so called "DRY" series, referring to the curing conditions in the laboratory. These curing conditions resulted from the practical problems connected to storage of the largest specimens in the climate room. In order to check the effect of differential shrinkage of the specimens in relation to the specimen size, a second series of experiments on concrete specimens was conducted. Contrary to the "DRY" series, this "WET" series comprised specimens of types **A**, **B**, **C** and **D** which were cured in the climate room under controlled conditions (20°C, 95% R.H.). Consequently, also the procedure for the specimen preparation as described above differed for the specimens of the WET series. The day prior to testing the specimens were taken out of the climate room, wrapped in a wet cloth and covered with plastic. The ends of the specimen were left free to enable the glueing of the loading platens. At the day of testing the plastic was cut away locally to allow for glueing the measuring points. The remaining foil and wet cloth was removed directly before the start of the test.

2.3.2 Sandstone

In the quarry, the sandstone specimens were machined in their final shape, i.e. with the same geometry as the concrete specimens. After arrival the specimens were stored in the laboratory to dry out.

For the specimens of types **A** to **C** this drying period was 7 weeks, increasing to more than 13 weeks for the largest specimens. The remaining preparation of the sandstone specimens was identical to the procedure as described for the DRY concrete series.

2.4 *Measurements*

The size effect experiments that are found in the literature mainly focus on the peak load and failure strength, rather than the complete post-peak behaviour and (differences in) crack mechanisms between the various specimen sizes. Perhaps the only exception are the tests performed by Ferro (1994), although the size range was limited there to 1:8. In the present study it was attempted to fill this gap by closely monitoring the fracture behaviour of the concrete and sandstone during the test. For this purpose a measurement scheme has been designed that was applied for all specimens.

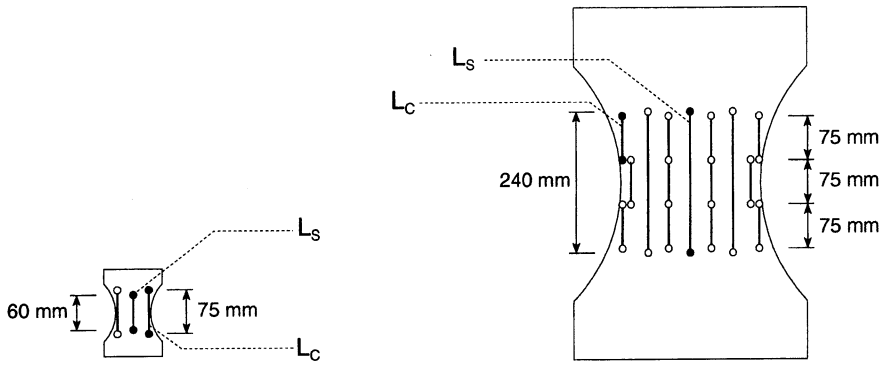

(a) type ***B*** *(b) type* ***D***

Fig. 2. Placement of displacement transducers on specimen type ***B*** *(a) and* ***D*** *(b).* L_c *refers to constant control measuring length;* L_s *to scaled measuring length.*

The scheme basically consisted of 2 types of measurements, namely those needed for test control and additional measurements that would give insight in the process of crack propagation. As mentioned before, LVDTs with a constant measuring length of 75 mm were placed along the edges of a specimen. These LVDTs were used to control the test. The number of control LVDTs varied with the size of the specimen. As is shown in Fig. 2, one LVDT at each edge sufficed to perform a test on a specimen type **B** (Fig. 2a) whereas three LVDTs were placed along each edge of a specimen type **D** (Fig. 2b). Furthermore, in the area covered by the control LVDTs, additional LVDTs with the same measuring length of 75 mm were placed over the specimen width. With these latter LVDTs the propagation of the crack through the specimen could be followed. Apart from these measurements with constant measuring length, also measurements with a measuring length scaled according to the specimen size were carried out (denoted by L_s in Fig. 2a,b). Hence the measurement covered the same part of the specimen independent of its size, thus allowing for mutual comparison of the measurements.

3 Experimental results

3.1 *Concrete tests (I): specimens stored in the laboratory ("DRY" series)*

At least four successful (i.e. with a *complete* softening curve) tests were conducted for each specimen size. All force-deformation curves are shown in Fig. 3a and b, where the deformation is the average deformation of the scaled measurements Ls on the front and the back side of a specimen (Fig. 2). The measured forces have been corrected for the dead weight of the upper loading platen and the part of the specimen above the crack. The weight of the specimen part below the crack, the lower loading platen and the lower hinge construction are incorporated in the measured force and can be seen as a constant, uncontrollable part of the external load. The tests were conducted with a deformation rate of 0.028 μm/s and continued until the first control LVDT exceeded its measuring range, which was at 500 μm. Because of the large width of the **E** and **F** specimens however, this meant that still a residual strength of approximately 15% of the ultimate load was present at the moment the test was stopped.

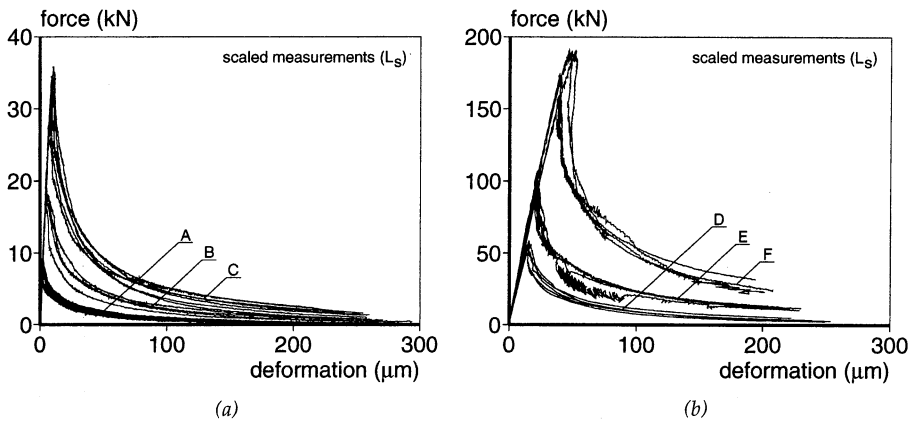

*Fig. 3. Overview of the force-deformation curves for specimens **A**, **B**, **C** (a) and **D**, **E**, **F** (b) (DRY series).*

In Fig. 3b, the effect of using a constant, small control length L_c (Fig. 2) can be seen. The softening curves of the type *F* specimens, which show a clear snap-back behaviour, could not have been retrieved if the scaled measuring length had been used to control the test. Because of the large elastic deformations within L_s the measured deformation decreases after peak load.

Table 2. Mean values for the nominal strength and the fracture energy of the concrete tests of the DRY series. G_F is based on the average scaled measurements.

		σ_N [MPa]		G_F [N/m]
type	number	mean (std.dev.)	number	mean (std.dev.)
A	10	2.54 (0.41)	9	97.0 (11.8)
B	4	2.97 (0.19)	4	125.7 (18.0)
C	7	2.75 (0.21)	7	124.2 (13.6)
D	5	2.30 (0.09)	5	125.2 (13.7)
E	4	2.07 (0.12)	4	142.3 (10.3)
F	4	1.86 (0.16)	4	141.1 (10.2)

To assess the size effect on strength in the present tests, the nominal strength σ_N ($= F_u / 0.6bD$) has been computed for each test. The results are shown in Fig. 4a and Table 2. Apart from a clear size dependence of the nominal strength, a strong scatter is observed in the results of the type **A** specimens, which covers almost the entire band width in which all the other test results (i.e. for larger sizes) are lying. Apart from the large scatter it is found that the average nominal strength for the type **A** specimens is lower than for the type **B** specimens (Table 2). Both observations indicate that the aspect ratio of D/d_{max} for the type **A** specimens is too small, leading to a too small specimen volume compared to the representative volume. As a consequence the ultimate load of a test can be strongly influenced by wall effect and by stress concentrations due to the presence of large aggregates in the smallest cross section. It is mentioned that the larger scatter in the strength values of the smallest specimens also follows from numerical simulations with a lattice model (Van Vliet, 2000), as well as from other experiments (e.g. Kadleček and Špetla, 1967). Hence, the results suggest that for concrete the size of the representative volume should be taken larger than 3.75 d_{max}, perhaps even as large as 6–7 d_{max}. Moreover, this finding questions the practical use of discussions about strength asymptotes in models that describe size effect on nominal strength for very small specimen sizes.

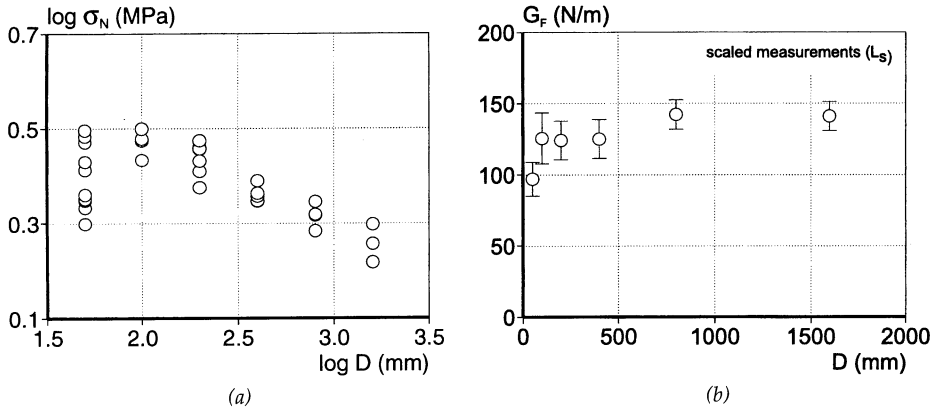

Fig. 4. Nominal strength (a) and fracture energy (b) versus size (DRY series).

For the fracture energy G_F, which is based on the average scaled measurements L_s on the front and the back size of a specimen (Fig. 2), the definition by Hillerborg (1985) has been adopted. The pre-peak energy dissipation has been subtracted for the specimens of all types, to avoid differences in the fracture energy due to the increasing measuring length up to 960 mm for the type **F** specimens. Note however, that the contribution of this pre-peak energy dissipation to G_F appeared to be limited to a maximum of 3% for the largest specimens. The presented values of G_F have been computed by linearly extrapolating the tail of the softening curves until intersection with the x-axis.

With exception of the smallest specimens, the variation of G_F with size is limited (Fig. 4b and Table 2) and disappears for larger specimen sizes. This could indicate that the relative amount of damage that develops during crack propagation is not strongly correlated with the size. Any observation with respect to G_F is made within the limitation of the constant specimen thickness, which for larger specimens could lead to values for the fracture energy that are too low.

3.2 *Concrete tests (II): specimens stored in the climate room ("WET" series)*

In the second series of concrete tests, the WET tests, the same deformation rate was applied as in the DRY series and also the data correction was carried out in a similar manner. The nominal strength values which were found in the WET series were quite different compared to those of the DRY series. In fact, apart from the **D** specimens the ultimate loads for all other types of specimens were lower (see Fig. 5a and Table 3) and σ_N was found to increase rather than decrease with size. In the WET tests, moisture can have had two, counteracting, influences. Because of the 95% humidity moisture condition in the climate room, the WET specimens will have hydrated better compared to the DRY specimens, resulting in a higher strength. Since the moisture content of the WET specimens was higher at the time of testing than the moisture content of the DRY specimens, the strength will have been lower as is known from literature. Yet, a comparison of the results of the type **D** specimens of the DRY and the WET series shows that both influences might have been comparable.

A third moisture effect, which is likely to have played a role in the WET tests, is the development of eigen-stresses due to differential drying out after the specimens had been taken out of the climate room (see also Bonzel and Kadleček (1970) and Hordijk (1991)). Despite the fact that the specimens were wrapped in wet cloth and covered by plastic to prevent drying out, these measures might not have been sufficient. Eigen-stresses would have the most significant effect on the behaviour of the small specimens because of their large specific area. For the **D** specimens only a small part of the cross section will dry out, meaning that the effect of eigen-stresses will be negligible. This could be the explanation for the similar strength values of the type **D** specimens from both the WET and the DRY series. Following this line of reasoning would also imply that for specimens larger than type **D**, the WET series might show the same size effect on strength as was found for the DRY series.

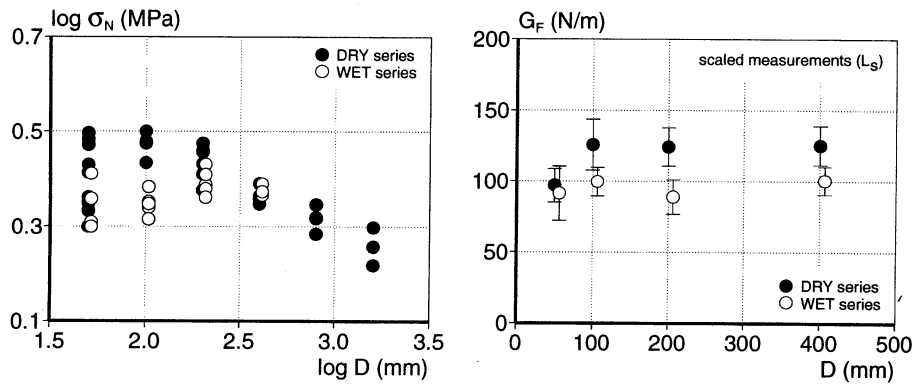

Fig. 5. Nominal strength (a) and fracture energy (b) vs. size for DRY and WET series.

Table 3. Mean values for the nominal strength and the fracture energy of the concrete tests of the WET series. G_F is based on the average scaled measurements.

		σ_N [MPa]		G_F [N/m]
type	number	mean (std.dev.)	number	mean (std.dev.)
A	5	2.17 (0.25)	5	91.5 (19.2)
B	5	2.23 (0.13)	5	99.6 (10.1)
C	5	2.48 (0.16)	5	88.9 (12.1)
D	4	2.37 (0.06)	3	100.4 (9.9)

The results that were found for the fracture energy of the specimens in the WET series are presented in Fig. 5b and Table 3. Apart from the results of the type **A** specimens, the variation of G_F with size is consistent with the findings in the DRY series. The absolute values for G_F in the WET series however, are lower compared to the DRY series. This can be attributed to a larger amount of micro-cracks that developed during the shrinkage process that took place in the specimens of the DRY series after they were stored in the laboratory. Due to these micro-cracks first of all more macro-cracks will develop. In addition, the macro-cracks will branch rather than going straight through the specimen's cross section. Both mechanisms will lead to a higher value for the fracture energy.

3.3 *Sandstone tests*

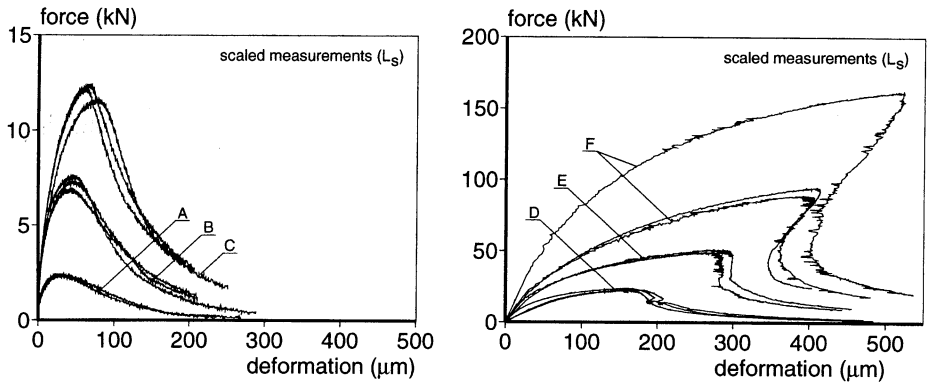

Fig. 6. Overview of force-deformation curves for the sandstone specimens.

The sandstone specimens that have been tested were delivered in their final shape, directly from the quarry in Germany. For each size three specimens were available. After testing the specimens of types **A** to **C** it appeared that the maximum range of the LVDTs, which was 500 μm, was rather small because of the large deformational capacity of the sandstone (compare Fig. 6 and Fig. 3). The measuring range of the LVDTs was therefore changed to 1000 μm for the testing of specimen types **D** to **F**. All tests were conducted with a deformation rate of 0.056 μm/s. In Fig. 6 an overview is given of the recorded force-deformation curves, where the deformation is again based on the average value of the scaled measurements in the middle of the specimen. Due to problems with one of the two LVDTs a curve from a test on an **E** specimen is missing, although the ultimate load for this test has been recorded. A comparison between Fig. 6 and Fig. 3 learns that the sandstone behaves completely different from concrete. The material has a lower stiffness, is weaker and shows a much higher pre-peak non-linearity compared to concrete. Despite the fact that the sandstone is a natural material the reproducibility of the tests was rather good, which can be attributed to the homogeneous material composition. Only for specimen types **E** and **F** one out of three tests for each type showed deviant behaviour, which is commonly observed in rock testing (Schlangen and Van Mier (1995), Wijk et al. (1978)). As a result a strength was found that was much higher compared to the other two specimens of the same dimension. In Fig. 7a the strength values of the sandstone speci-

mens are shown. The recorded strength of the two **A** specimens was remarkably low, whereas for the **E** and the **F** specimens two extremely high strength values were found. Although a special request was made for manufacturing specimens out of the same block of sandstone, it can not be ascertained that this has actually been the case. This doubt is supported by additional tests on the remains of the high strength **E** and **F** specimen, which confirmed that the material differed from that of the other dog-bone specimens. The layered composition of the red Felser sandstone, as well as the possible presence of faults and weak spots, can explain the low strength of the **A** specimens. Specimens of larger sizes will be less sensitive for the presence of such local inhomogeneities. Local inhomogeneities in a small specimen on the other hand, will govern the experimental result and in this case the ultimate strength that is found. When supposing that the high strength **E** and **F** specimen are outliers, the mean strengths for the largest specimens are comparable to those found for the smaller specimens (Table 4). Hence, the size effect found in the sandstone tests seems to vanish for specimen sizes larger than type **C**.

Table 4. Mean values for the nominal strength and the fracture energy of the sandstone tests. G_F is based on the average scaled measurements.

type	number	σ_N [MPa] mean (std.dev.)	number	G_F [N/m] mean (std.dev.)	G_F^* [N/m] mean (std.dev.)
A	2	0.82 (-)	2	76.7 (-)	92.6 (-)
B	3	1.22 (0.06)	3	111.3 (3.7)	147.0 (3.8)
C	3	1.01 (0.03)	3	93.8 (4.4)	136.2 (3.2)
D	3	0.96 (0.03)	3	135.1 (13.0)	208.1 (17.6)
E	2	1.04 (-)	2	143.3 (-)	299.6 (-)
F	2	0.96 (-)	2	93.2 (-)	291.1 (-)

The fracture energy G_F for the sandstone specimens has, just like for the concrete specimens, been computed using the average scaled measurements in the middle of the specimen. At first, Hillerborg's definition was adopted thereby subtracting the pre-peak inelastic or bulk energy from the total energy. In Fig. 7b it can be seen that because of this starting point the computed total energy is strongly reduced, which has been illustrated by introducing G_F^*. This alternative fracture energy represents the total area under the stress-deformation curve and thus takes into account bulk energy dissipation as well. The latter definition implies, however, that the pre-peak non-linearity must be irreversible and due to micro-cracking in the vicinity of the final crack. Whether this condition is actually fulfilled, even in the tests on the **F** specimens where the measuring length measured 960 mm, can not be deduced from the available results. It is mentioned that the decrease of the fracture energy for the **F** specimens is believed to be artificial, and due to the fact that the tests on those specimens had to be stopped relatively early. As a result, the linearly extrapolated descending branch of the σ - w relation, which was used to compute the fracture energy, intersects the x-axis at

a deformation which is probably too small. It is expected however, that in the end the fracture energy converges towards a constant value. Note that despite the small grain size of the sandstone, apparently a very large ratio between minimum specimen dimension and maximum grain diameter has to be maintained before this plateau is reached.

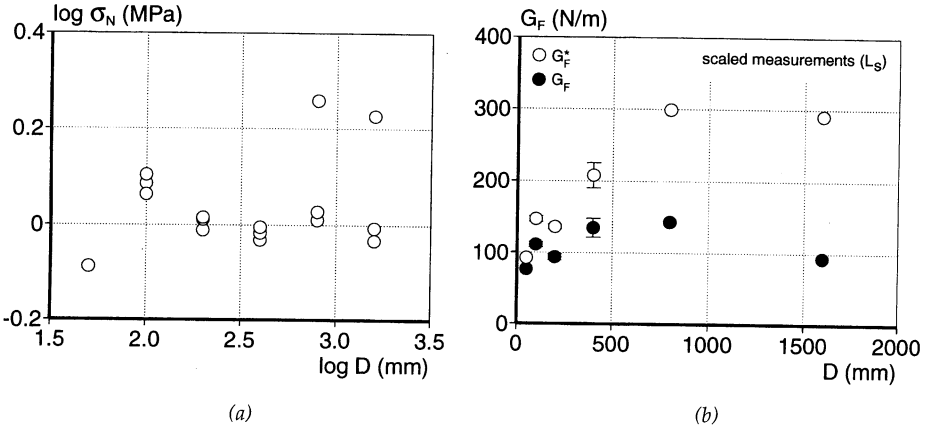

(a) (b)

Fig. 7. Nominal strength (a) and fracture energy (b) vs. size for the sandstone specimens.

4 Discussion on the size dependence of the concrete strength

4.1 *General explanations for size effect in unnotched structures*

When stress redistributions and non-linearity of deformations play a minor role in the failure of a material, failure of this material can be seen as a statistical phenomenon. In other words, the ultimate load that can be transferred depends on the distribution of flaws within the material. Whenever the strength of the weakest spot is exceeded, the ultimate load has been reached and the material fails. This type of material failure is described by Weibull's theory (Weibull, 1939), also known as the weakest link theory. In literature, size effect of concrete under uniaxial tensile loading conditions is mostly attributed to this type of failure, which is also called statistical or material size effect. If on the other hand the stress distribution in the cross section of a specimen is non-uniform, such as in bending states, the explanation of size effect in concrete is based on the increasing relative crack length at comparable load levels (relative to peak load), for specimens of increasing size. This phenomenon, in combination with the softening behaviour of concrete, leads to a decrease of the nominal strength with size as was shown in numerical simulations by Hillerborg and co-workers (Hillerborg et al., 1976). Contrary to statistical size effect this latter type of size effect is deterministic. It is referred to as structural or energy-based size effect, and has as typical feature that stress-redistributions are still possible after the tensile strength has been exceeded, which also explains why the external load can still increase after localised cracking has occurred. For specimens up to a certain size structural size effect is used to explain the fact that the bending strength is higher than

the uniaxial tensile stress. For large specimens with small strain gradients however, this difference disappears and the bending strength approaches the uniaxial tensile strength.

4.2 *Observations in the present experiments*

In the present experiments, at peak load tensile stresses act in the entire cross section. From this point of view the observed size effect on strength should be a Weibull type, which seems to be confirmed by Fig. 8a. There, the average nominal strength values are presented per specimen size, and the straight line presents the size effect according to Weibull theory, which can be shown to follow a slope of approximately 1:6 in a bi-logarithmic plot of σ_N vs. D (Van Vliet and Van Mier, 1999). Note that the slope of the Weibull relation is related to the coefficient of variation (V) of the experimentally found strength values through $1{:}1/(nV)$, where n stands for the number of dimensions. For two-dimensional similarity $n = 2$, and together with the average value of V for the strength results of the DRY series (Table 2), a slope is found of approximately 1:6. This could indicate that a Weibull type of size effect is dominant for the present experiments. However, if the size effect in the present experiments would be purely statistical, first of all the conditions for the occurrence of this type of size effect (uniform state of stress, no stress redistributions) would have to be met. Secondly, the Weibull relation would have to apply to the results of the tests of both the DRY and the WET series, which is not the case as can be seen in Fig. 8b. In concrete, stress redistributions and thus progressive failure will always occur to some extent. The degree of stress redistributions dependends on among others the state of stress. Hence, applying Weibull theory to concrete failure would already involve a more advanced kind of Weibull theory, compared to the original version which purely deals with instant failure of the complete structure. As for the application of Weibull's relation to the results of the WET series, Fig. 8b shows that no agreement can be found. If a statistical or material size effect is present, then it is completely overruled by other, possibly structural, effects which appeared during the tests.

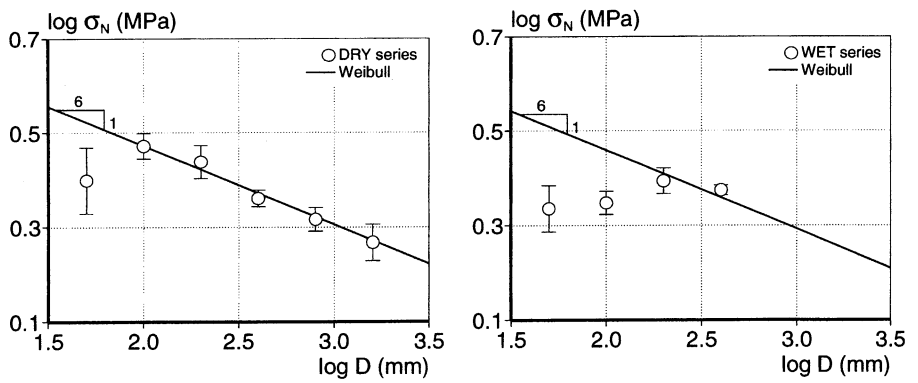

Fig. 8. Comparison between Weibull theory and results of DRY series (a) and WET series (b) respectively.

A detailed analysis of the experiments revealed that at peak load, the actual deformation state in the cross section of the dog-bone shaped specimens was far from uniform. These non-uniform deformations could be attributed to:

- the shape of the specimens;
- the eccentricity of the external load;
- material inhomogeneity over the cross section of a specimen;
- eigen-stresses due to differential shrinkage.

Whereas the effect of specimen shape and load-eccentricity are relatively transparent, this may not be the case for stiffness differences over the specimen thickness, which were caused by segregation effects during casting. Due to these stiffness differences the centre of stiffness and the centroid of the cross section do not coincide anymore, leading to strain gradients over the cross section. Note that these strain gradients occur even if the external load is applied centrically in the out-of-plane direction. In presence of the aforementioned effects the crack generally initiates at a corner of the specimen.

4.3 *Analytical model to link non-uniform deformations and size effect*

The deformation gradients that occurred in the experiments were unique for each specimen. To get insight in their effect on the ultimate load that had been recorded in a specific test, a simple analytical model was derived. The basic idea behind the model is that predictions can be made for the ultimate load of each experiment, by using the initial deformation measurements as input for the model. By comparing the predicted ultimate load values with the values which were actually recorded in the experiments, the influence of the deformation gradients becomes more transparent. Here, only the general aspects of the model will be addressed whereas for a detailed derivation, the reader is referred to (Van Vliet and Van Mier (1999), Van Vliet (2000)).

In the model, the homogeneous specimen is assumed to follow Bernoulli beam theory (i.e. plane sections remain plane), and failure is assumed to take place in the smallest cross section. The stress-strain relation in this cross section is defined by Hooke's law, leading to failure of the specimen as soon as the critical stress σ_{crit} is reached in any point. This critical stress, which can be regarded as the local material strength, is arbitrarily set and constant for all specimens. To compute the critical stress σ_{crit}, the strain distribution in the smallest cross section (parallel to the $x-z$ plane) is defined as

$$\varepsilon(x,z) = \varepsilon_{ax} + \kappa_z x + \kappa_z z$$

where ε_{ax} stands for the axial strain in the centre of curvature and κ_z and κ_x represent the curvature of the specimen in the $x-y$ and $z-y$ plane respectively. According to this model, the highest strain will be found in one of the corners in the middle of the specimen. Through the Young modulus of the specimen, σ_{crit} can be computed from the highest strain. The only missing information concerns the Young modulus E and the curvatures in the in-plane and out-of-plane direction, κ_z and κ_x, respectively. These were all three computed from the deformation measurements which were made in the laboratory experiments. Crucial is, that for the computation of κ_z and κ_x deformations were

used at approximately 30% of peak load. With increasing load, κ_z and κ_x were assumed to vary linearly with the external load F thereby neglecting non-linear deformations. Hence, the ultimate load F_u at which σ_{crit} was reached could be directly computed.

The model which has been described before, has been applied to the concrete experiments of the DRY and the WET series. In Fig. 9a and b the mean values and standard deviations of the model calculations are compared with the experimentally measured nominal strength values for both test series.

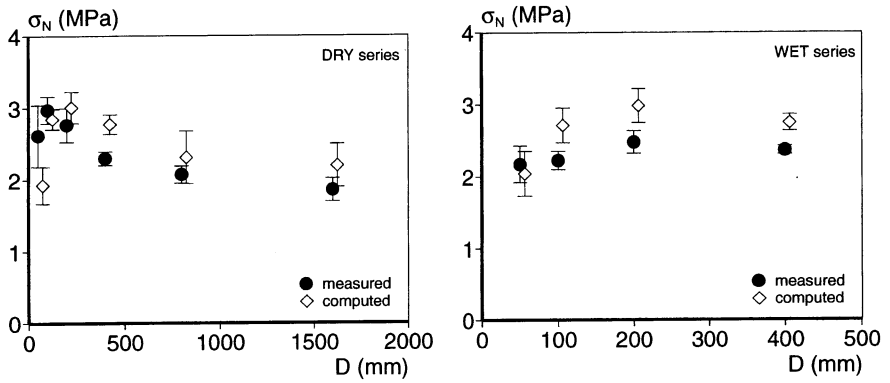

(a) *(b)*

Fig. 9. Mean values of measured and computed nominal stresses for the DRY series (a) and the WET series (b).

Keeping in mind that the value for σ_{crit} was set rather arbitrarily, the mutual differences between σ_N values of different specimen sizes must be compared for the model as well as the experiments. The absolute difference between the model values and the experimental values is variable, since the magnitude of the model values directly depends on the applied value for σ_{crit}, and can therefore vary. In case of the DRY series (Fig. 9a), the model calculations agree fairly well with the global response of the experiments. For the small specimen sizes the correct trend is found: a decrease of the nominal strength is calculated, although the decrease appears to go too rapid. In this respect the results for the WET series seem to be in better agreement (Fig. 9b), since also for the type **B** specimens a relative strength level is found which is in accordance with that of the experiments. The nominal strength of the **A** specimens is again far too low.

A general observation is that for the smallest specimens, the model overestimates the effect of the strain gradients (curvatures) on the ultimate load. This can be explained by the absence of a material structure in the model, which in reality could overrule the influence of strain gradients for specimens with dimensions close to, or smaller than the representative volume (Heilmann, 1976). For larger specimen sizes this effect disappears. Further elaboration revealed that no relation was

present between the magnitude of the occurring strain gradients and the specimen size, whereas the nominal strength which was found decreased with increasing strain gradient (Van Vliet, 2000). If only moderate strain gradients were present in a test, the occurring size effect was a material type of size effect and thus governed by statistical aspects. This latter finding was confirmed by numerical simulations, in which the uniaxial tension tests on dog-bone shaped specimens were simulated with a lattice model (Van Vliet, 2000).

5 Conclusions

Through a combination of experiments, numerical simulations and an analytical model, the effect of stress and/or strain gradients on size effect of concrete could be clarified. These gradients were found to be introduced by the shape of the specimens, the eccentricity of the external load, inhomogeneity of the specimen's cross section and eigenstresses due to differential drying. Hence, in the experiments on concrete specimens, three different causes could be distinguished for the observed size effect. In the smallest specimens the failure stress was governed by the concrete aggregate structure. With increasing size of the specimens, the role of the statistical strength distribution increased as well. The presence of flaws in the concrete therefore determined the ultimate stress, unless stress and/or strain gradients of a structural nature were present in the specimens, which were strong enough to overrule these material size effects. Therefore, size effect on strength can not be fully understood unless the material composition and the specimen geometry, as well as the presence and magnitude of stress and/or strain gradients is considered.

Contrary to the concrete tests, the size effect on the nominal strength that was found in tests on red Felser sandstone appeared to be very mild and vanished already for specimens of the third size.

The fracture energy was, irrespective of the type of material, found to increase with size going towards a horizontal asymptote for large sizes. Although for concrete the variation of the fracture energy with size was independent of the curing conditions, the highest values were found for the specimens cured under dry conditions.

From experiments as well as numerical simulations followed that for the smallest concrete specimens used in this study, the aspect ratio of $D/d_{max} = 3.75$ was too small. As a consequence the results showed a strong scatter. An implication of this observation is that discussions about a strength asymptote for very small specimen sizes as used in some size effect models, do not seem to be of any practical interest.

Acknowledgements

The authors wish to thank Mr. Gerard Timmers for his expert assistance in conducting the experiments and solving numerous technical problems. The research was financially supported by the Dutch Technology Foundation (STW), which is gratefully acknowledged.

References

BAŽANT, Z.P. SCALING of quasibrittle fracture: Asymptotic analysis, *Int. J. of Frac.*, 1997, 83(1), pp. 19-40.

CARPINTERI, A., CHIAIA, B. and FERRO, G. Multifractal scaling law for the nominal strength variation of concrete structures. In M. Mihashi, H. Okamura, and Z.P. Ba_ant, editors, *Size effect in concrete structures.* E&FN Spon, London/New York, 1994, pp. 173-185.

BONZEL, J. and KADLEČEK, V. Einfluss der nachbehandlung und des Feuchtigkeitszustands auf die Zugfestigkeit des Betons. In K. Walz, editor, *Betontechnische Berichte 1970*, 1970, pp. 99-132 (in German).

FERRO, G. *Effetti di scala sulla resistenza a trazione dei materiali*, PhD thesis, Politecnico di Torino, Torino, Italy, 1994 (in Italian).

HEILMANN, H.G. Zugspannung und Dehnung in unbewehrten Betonquerschnitten bei exzentrischer Belastung, *DAfStb*, 1976, volume 269, pp.1-61 (in German).

HILLERBORG, A., MODÉER, M. and PETERSSON, P.-E. Analysis of crack formation and crack growth in concrete by means of fracture mechanics in finite elements, *Cem. and Con. Res.*, 1976, 6, pp. 773-782.

HILLERBORG, A. The theoretical basis of a method to determine the fracture energy GF of concrete, Mat. and Struct. (RILEM), 1985, 18 (106), pp. 291-296.

HORDIJK, D.A. *Local Approach to Fatigue of Concrete*, PhD thesis, Delft University of Technology, Delft, the Netherlands, 1991.

KADLEČEK, V. and ŠPETLA, Z. Effect of size and shape of test specimens on the direct tensile strength of concrete. *RILEM Bulletin*, 1967, 36, pp. 175-184.

LI, Z., KULKARNI, S.M. and SHAH, S.P. New test method for obtaining softening response of unnotched concrete specimen under uniaxial tension. *Exp. Mech.*, 1993, 9, pp.181-188.

SCHLANGEN, E. and VAN MIER, J.G.M. Crack propagation in sandstone: Combined experimental and numerical approach. *Rock Mech. and Rock Eng.*, 1995, 28(2), pp. 93-110.

VAN MIER, J.G.M., SCHLANGEN, E. and VERVUURT, A. Lattice type fracture models for concrete. In H.-B. Mühlhaus, editor, *Continuum models for Materials with Microstructure.* John Wiley & Sons Ltd., Chichester, UK, 1995, pp. 341-377.

VAN VLIET, M.R.A. and VAN MIER, J.G.M. *Uniaxial tension tests on red and yellow Felser sandstone*, Tech. Rep. 25.5-97-9, Delft University of Technology, Delft, the Netherlands, 1997.

VAN VLIET, M.R.A. and VAN MIER, J.G.M. Effect of strain gradients on the size effect of concrete in uniaxial tension, *Int. J. of Fracture*, 1999, 95(1/4), pp.195-219.

VAN VLIET, M.R.A. *Size effect in tensile fracture of concrete and rock.* PhD thesis, Delft University of Technology, Delft, the Netherlands, 2000.

WEIBULL, W. *A statistical theory of the strength of materials*, Royal Swedish Academy of Eng. Sci. Proc., 1939, 151, pp. 1-45.

WIJK, G., REHBINDER, G. and LOGDSTROM, G. The relation between the uniaxial tensile strength and the sample size for Bohus granite. *Rock Mech.*, 1978, 10, pp. 201-219.